

Supplementary Material

Immunomagnetic particles exhibiting programmable hierarchical flower-like nanostructure for enhanced separation of tumor cells

Na He,¹ Han Bao,^{2,3} Jingxin Meng,^{2,3} Yongyang Song,^{2,3*} Li-Ping Xu,^{1*} Shutao Wang^{2,3}

¹ Beijing Key Laboratory for Bioengineering and Sensing Technology, School of Chemistry and Biological Engineering, University of Science and Technology Beijing, Beijing 100083, P. R. China.

² CAS Key Laboratory of Bio-inspired Materials and Interfacial Science, Technical Institute of Physics and Chemistry, Chinese Academy of Sciences, Beijing, 100190, P. R. China.

³ University of Chinese Academy of Sciences, Beijing, 100049, P. R. China.

* Corresponding authors

E-mail address: yysong@mail.ipc.ac.cn (Yongyang Song),

xuliping@ustb.edu.cn (Li-Ping Xu)

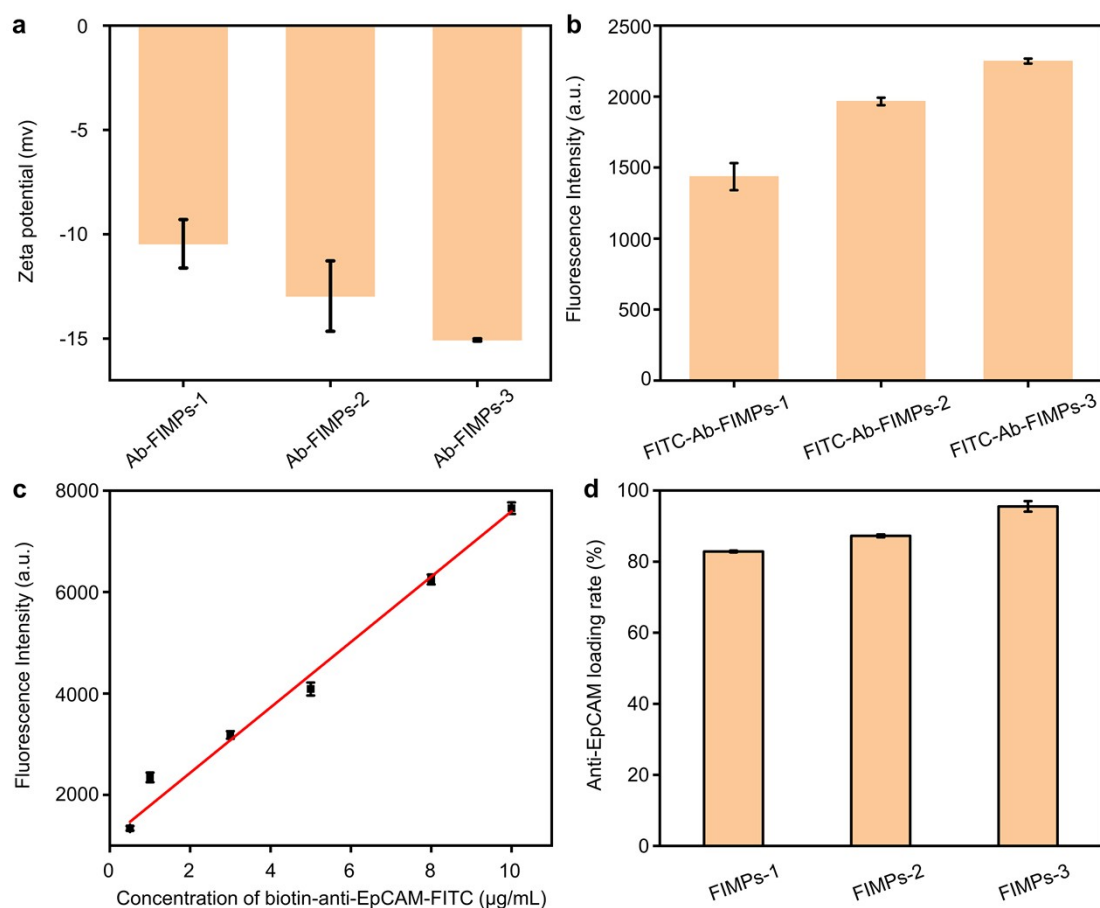


Fig. S1 (a) Zeta potential values of the Ab-FIMPs-1, Ab-FIMPs-2, and Ab-FIMPs-3. (b) Fluorescence intensity of FITC-Ab-FIMPs-1, FITC-Ab-FIMPs-2, and FITC-Ab-FIMPs-3. (c) The linear regression curve of the fluorescence intensity versus the concentration of biotin-anti-EpCAM-FITC. (d) The anti-EpCAM loading rate on FIMPs-1, FIMPs-2 and FIMPs-3.

Fluorescein Isothiocyanate (FITC) labeling. The biotin-anti-EpCAM solution (1 mg/mL) was mixed with Na_2CO_3 solution (0.1 M), and 10 μL of FITC solution (1 mg/mL), and maintained overnight at 4 $^\circ\text{C}$. The biotin-anti-EpCAM-FITC was rinsed for 5 ~ 8 times with PBS, and was then dissolved in 1 mL of PBS. To calculate the loading rate of anti-EpCAM on FIMPs-1, FIMPs-2, and FIMPs-3, different concentrations of biotin-anti-EpCAM-FITC (0.5, 1, 3, 5, 8, and 10 $\mu\text{g/mL}$) were prepared, and then fluorescence detection was performed to make a standard curve (Fig. S1c). FIMPs-1, FIMPs-2, and FIMPs-3 were incubated with biotin-anti-EpCAM-FITC for 45 ~ 90 min. The supernatant was removed after magnet adsorption and washed thrice with PBS. The fluorescence intensity detection experiments were then

performed. Finally, the loading rate of anti-EpCAM in FIMPs (Fig. S1d) was calculated from the standard curve. The weight proportion of anti-EpCAM on Ab-FIMPs-1, Ab-FIMPs-2, and Ab-FIMPs-3 are 0.56%, 0.59%, and 0.64%, respectively.

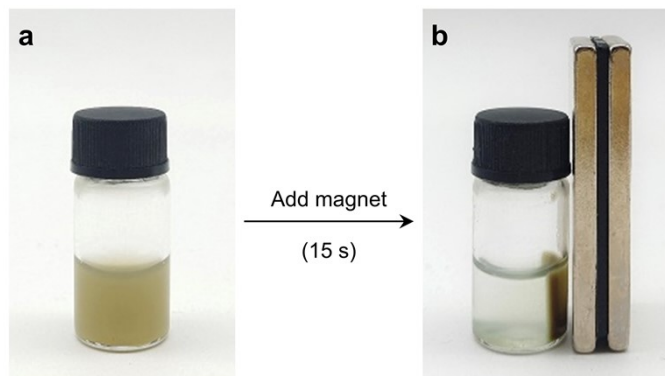


Fig. S2 Pictures of FIMPs before (a) and after (b) being adsorbed by magnets.

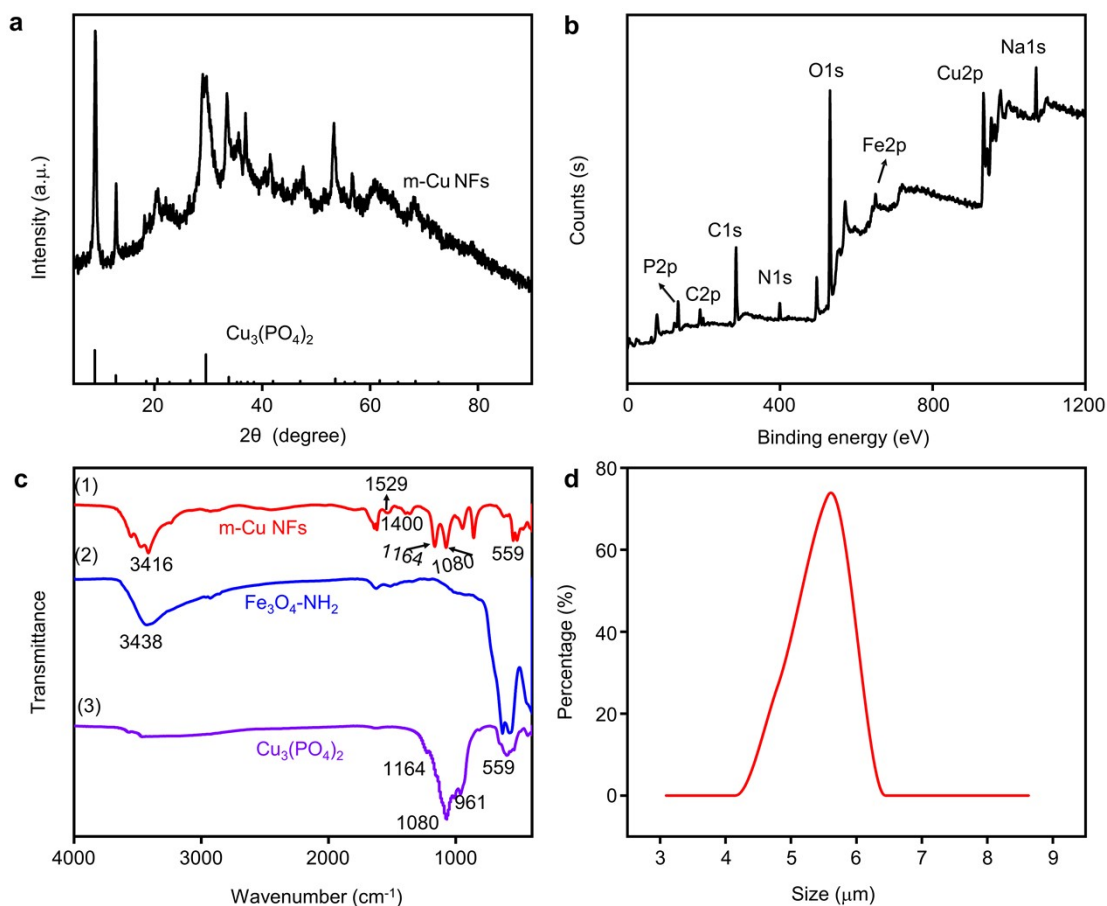


Fig. S3 (a) XRD patterns of FIMPs. (b) XPS mode of FIMPs. (c) FT-IR of FIMPs (1), $\text{NH}_2\text{-Fe}_3\text{O}_4$ (2), and $\text{Cu}_3(\text{PO}_4)_2$ (3). (d) Particle size distribution of FIMPs.

The X-ray powder diffraction (XRD) was performed to demonstrate the inorganic component of the FIMPs, and the X-ray diffraction pattern of the nanoflower power

matched well with that of $\text{Cu}_3(\text{PO}_4)_2 \cdot 3\text{H}_2\text{O}$ according to the JCPDS card (PDF#22-0548), which indicates that the inorganic composition of FIMPs is $\text{Cu}_3(\text{PO}_4)_2$. The X-ray photoelectron spectroscopy (XPS) spectra of the as-prepared nanomaterials displayed the composition of P, C, N, O, Fe, and Cu elements, indicating the successful synthesis of FIMPs. The chemical nanostructure of hybrid FIMPs was monitored by Fourier transform infrared spectroscopy (FT-IR). The chemical nanostructure of the hybrid FIMPs is shown in Fig. S3c, where the strong IR bands (spectrum (1) and (3)) at 559 cm^{-1} , $1080 - 960\text{ cm}^{-1}$, and 1164 cm^{-1} were attributed to P-O and P=O vibrations, which indicated the existence of phosphate groups. Where the strong IR bands (spectrum (1) and (2)) at $3200 - 3600\text{ cm}^{-1}$ were attributed to Fe-O vibrations, which indicated the existence of $\text{NH}_2\text{-Fe}_3\text{O}_4$. Compared to spectrum (2) and (3), the typical bands of protein for $-\text{NH}_2$ at $1400 - 1600\text{ cm}^{-1}$ were observed in spectrum (1), which indicates that SA is successfully immobilized in FIMPs. The dynamic light scattering (DLS) was performed to determine the particle size of FIMPs. The particle size of FIMPs shows normal distribution, and the average diameter is about $5.35\text{ }\mu\text{m}$.

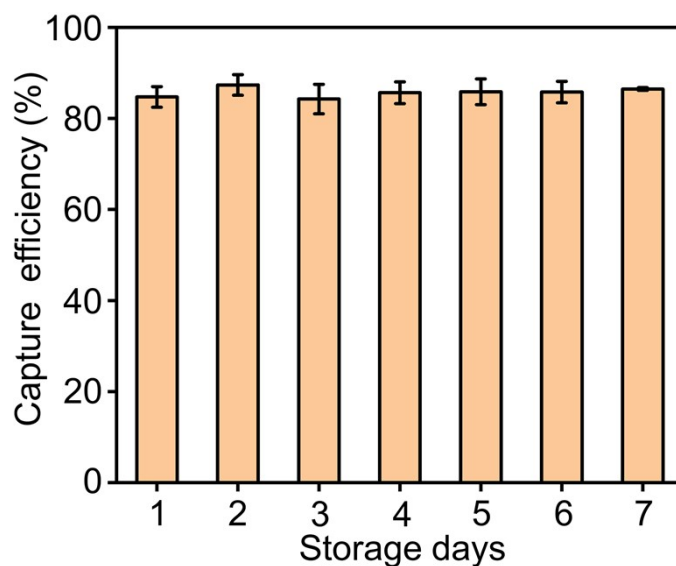


Fig. S4 Effect of Ab-FIMPs storage time on capture efficiency.

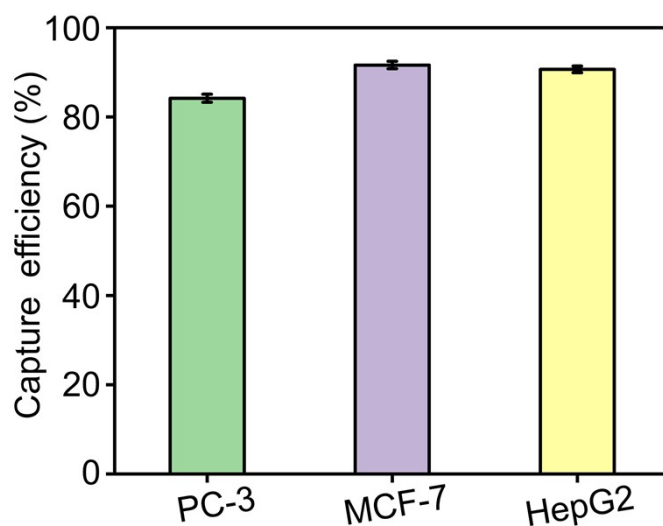


Fig. S5 The capture efficiency of different cells, including PC-3, MCF-7, and HepG2, when the cell concentration was 10^3 cells/mL. Data are presented as mean \pm standard deviation of three measurements.

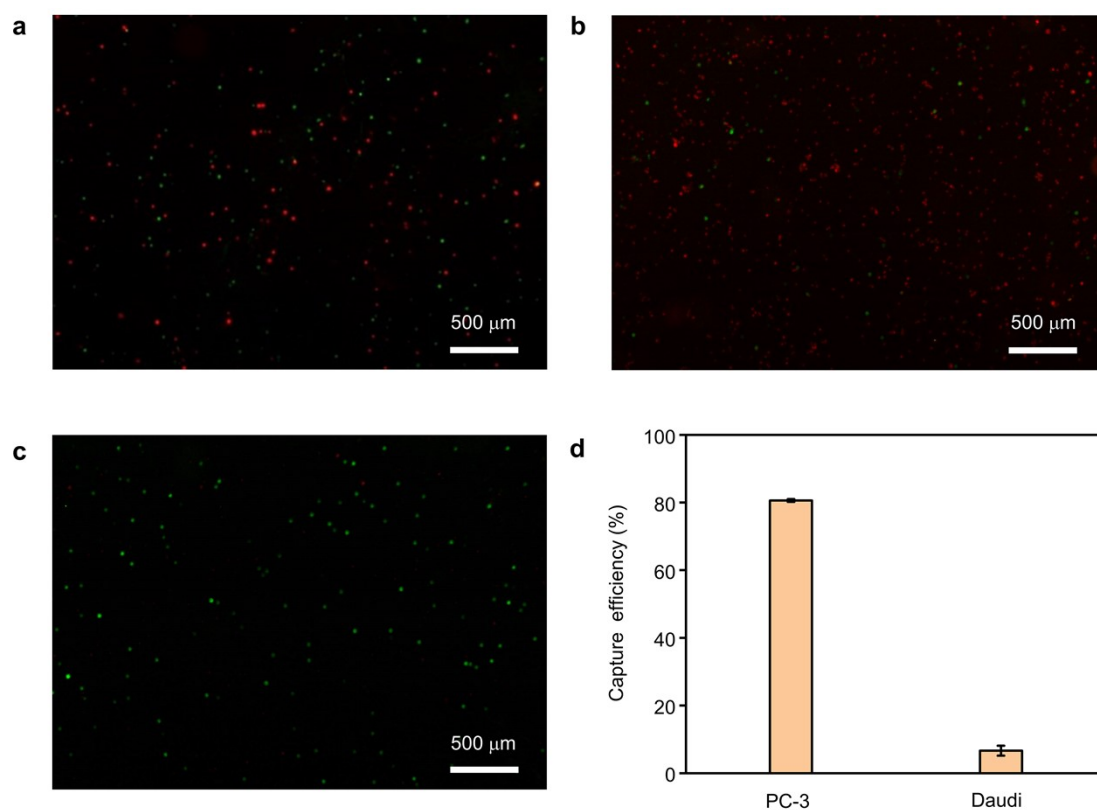


Fig. S6 (a) Fluorescence micrographs of the mixed cell suspension containing targeted PC-3 cells (green) and non-targeted Daudi cells (red) (1:1, 10^5 cells/mL). Fluorescence microscopy images of cells in the supernatant (b) and precipitate (c) after magnetic aspiration of the mixed cell suspension. (d) Effect of mixed cells on capture efficiency, PC-3 (5×10^4) was incubated with Daudi (5×10^4) in 1 mL of culture medium in an

incubator. Data are presented as mean \pm standard deviation of three measurements.

The performance of Ab-FIMPs in identifying and isolating target CTCs was tested by mixing target cell lines (PC-3 cells, dyed green) and non-specific cell lines (Daudi cells, dyed red). Both cell lines were mixed at the same concentration (5×10^4 cells/mL), and then loaded to Ab-FIMPs-3. Fluorescent images of cells in mixed solution with red and green color uniformly present. After incubation at 37 °C for 45 min, most cells in the supernatant fluoresced red. It showed that Daudi cells are mostly in the supernatant. In contrast, most cells in the precipitate fluoresced green, indicating that most of the cells in precipitation are PC-3 cells. The results showed that EpCAM-positive PC-3 cells are selectively captured onto Ab-FIMPs-3 with a high capture efficiency of $81.3\% \pm 2.5\%$, while the capture efficiency of EpCAM-negative Daudi cells is lower at $7.2\% \pm 3.5\%$.

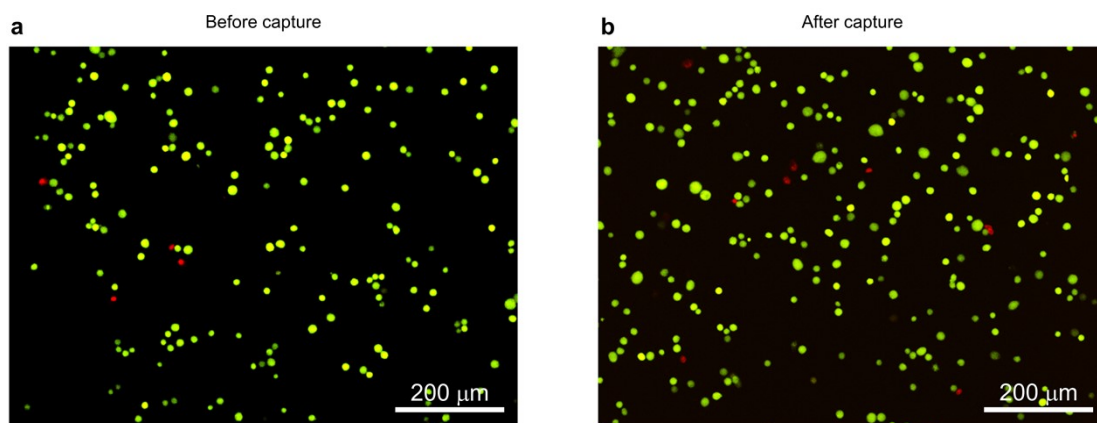


Fig. S7 (a) Fluorescence microscopic image of the cells before capture stained with calcein-AM (green) and propidium iodide (red). The cell survival rate is 97.9%. (b) Fluorescence microscopic image of the captured cells stained with calcineurin calcein-AM (green) and propidium iodide (red). The cell survival rate is 96.1%.

Table S1: Comparison of cell capture efficiency of FIMPs with existing materials.

Materials	Cell line	Sample	Capture efficiency	Reference
Alginate hydrogel	MCF-7	Rabbit whole blood	50.7%	<i>ACS Appl. Mater. Interfaces</i> , 2021, 13 , 19603–19612
TiO ₂ nanofiber substrate	PC-3	WBCs solution	70 ~ 80%	<i>Adv. Fiber Mater.</i> , 2020, 2 , 186–193

PEGylated boronate affinity cell imprinted polydimethylsiloxane (PBACIP)	SKBR3	Mice whole blood	46.7 ~ 65.3%	<i>Biosens. Bioelectron.</i> , 2023, 223 , 115023
Polystyrene (PS) nanosphere	HeLa	Whole blood from healthy volunteers	40 ~ 90%	<i>Anal. Methods</i> , 2019, 11 , 5718–5723
Microarray	MCF-7	Peripheral blood samples	63 ~ 74%	<i>Anal. Chem.</i> , 2020, 92 , 3403–3408
Cell-imprinted biomimetic interface	MCF-7	Rabbit whole blood	55 ~ 80%	<i>Biomater. Sci.</i> , 2019, 7 , 4027–4035
Magnetic graphene oxide	MCF-7	Human blood samples	78%	<i>J. Colloid Interf. Sci.</i> , 2023, 631 , 55–65
Hydrogel nanoparticles	MCF-7	WBCs solution	84%	<i>Colloid Surface. B.</i> , 2021, 202 , 111669
Flower-like immunomagnetic particles (FIMPs)	MCF-7	Lysed blood	86.4%	This work
	PC-3	Lysed blood	82.05%	
	MCF-7	Whole blood from healthy volunteers	83.4%	
	PC-3	Whole blood from healthy volunteers	79.15%	